Electron-impact excitation and ionization of H_2^+ using a configuration-average distorted-wave method

M. S. Pindzola, F. Robicheaux, and J. A. Ludlow
Department of Physics, Auburn University, Auburn, Alabama 36849, USA

J. Colgan
Theoretical Division, Los Alamos National Laboratory, Los Alamos, New Mexico 87545, USA

D. C. Griffin
Department of Physics, Rollins College, Winter Park, Florida 32789, USA
(Received 13 April 2005; published 25 July 2005)

A configuration-average distorted-wave method is developed to calculate electron-impact excitation and ionization cross sections for diatomic molecules and their ions. The method is based on the construction of bound and continuum orbitals on a two-dimensional numerical lattice in (r,θ) center-of-mass polar coordinates. Our first applications are the calculation of $1s\sigma \rightarrow 2p\sigma$ and $1s\sigma \rightarrow 2p\pi$ excitation cross sections and $1s\sigma \rightarrow \epsilon l\lambda$ ionization cross sections for H_2^+. Comparisons are made with plane-wave Born, distorted-wave, and *R*-matrix calculations, as well as experimental measurements.

DOI: 10.1103/PhysRevA.72.012716 PACS number(s): 34.50.Gb

I. INTRODUCTION

Electron collisions with molecules and their ions are important in many different areas of physics and chemistry, with a number of applications, including global climate studies, infrared and visible astrophysics, and studies of radiation damage to biological systems. In particular, resonance electron collisions with H_2, HD, and D_2 are important in understanding divertor plasma dynamics in controlled fusion experiments [1]. Over the years many theoretical and computational methods have been developed to treat electron-molecule collisions [2]. For example, in the last year the *R*-matrix approach for electron-molecule scattering has been extended to include continuum pseudostates [3] and finite elements [4]. The molecular time-dependent close-coupling method for double photoionization [5] is currently being extended to include electron-molecule collision processes. For these computationally intensive nonperturbative methods, it is important to also develop perturbative distorted-wave methods, so that a smooth transition can be made from low to high angular momenta and from low to high incident electron energies.

The semirelativistic configuration-average distorted-wave method [6] was originally developed to calculate electron-impact excitation, ionization, and recombination cross sections for complex atoms. In recent years, the configuration-average distorted-wave predictions for direct and indirect ionization cross sections along isonuclear sequences in heavy atoms have been found to be reasonably accurate when compared to crossed-beam experimental measurements [7–10]. A fully relativistic configuration-average distorted-wave method [11,12] was also developed to calculate electron-impact excitation and ionization cross sections for highly charged atomic ions. In general, the configuration-average distorted-wave method provides a rapid means of obtaining a fairly accurate estimate of electron-atom scattering cross sections and, as such, acts as a guide for more computationally demanding level-resolved perturbative distorted-wave and nonperturbative *R*-matrix calculations.

In this paper we develop a configuration-average distorted-wave method to calculate electron-impact excitation and ionization cross sections for diatomic molecules and their ions. As such, it will act as a guide in the application of the molecular time-dependent close-coupling method [5] to electron-molecule scattering. The distorted-wave method is based on the construction of bound and continuum orbitals on a two-dimensional numerical lattice in (r,θ) center-of-mass polar coordinates. In particular, the continuum orbitals are found by numerical solution of a elliptic partial differential equation, similar to the equation solved earlier in studies of electron-impact elastic scattering from H_2 [13] and the photoionization of H_2^+ and H_2 [14,15]. As a first test case, we apply the configuration-average distorted-wave method to the calculation of excitation and ionization cross sections for H_2^+. The inelastic cross sections are compared with atomic distorted-wave [6], molecular plane-wave Born [16], molecular distorted-wave [17], and molecular *R*-matrix [18] calculations, as well as experimental measurements [19,20]. Section II formulates the configuration-average distorted-wave method for diatomic molecules, Sec. III presents excitation and ionization cross section results for H_2^+, and a brief summary is given in Sec. IV. Unless otherwise stated, we will use atomic units.

II. THEORY

A. Configuration-average excitation

The most general excitation transition between configurations of a diatomic molecule is of the form

$$(n_1 l_1 \lambda_1)^{w_1+1}(n_2 l_2 \lambda_2)^{w_2-1} \epsilon_i l_i \lambda_i \rightarrow (n_1 l_1 \lambda_1)^{w_1}(n_2 l_2 \lambda_2)^{w_2} \epsilon_f l_f \lambda_f, \tag{1}$$

where n is the principal quantum number, l is the angular quantum number, $\lambda = |m|$ is the absolute value of the magnetic quantum number, w is the occupation number, $\epsilon_i = k_i^2/2$ is the incident electron energy, and $\epsilon_f = k_f^2/2$ is the final electron energy. The configuration-average excitation cross section is given by

$$\sigma_{exc} = \frac{32\pi}{k_i^3 k_f} \frac{(w_1+1)[S(\lambda_2)+1-w_2]}{S(\lambda_1)S(\lambda_2)} \times \sum_{l_i} \sum_{\lambda_i} \sum_{l_f} [M_d(f2;i1) + M_x(2f;i1) - M_c(f2/2f;i1)], \tag{2}$$

where $S(\lambda) = 2(2-\delta_{\lambda,0})$ is the total statistical weight of the $(nl\lambda)$ orbital and the continuum normalization is chosen as one times a sine function. The scattering terms M are defined in Sec. II C.

B. Configuration-average ionization

The most general ionization transition between configurations of a diatomic molecule is of the form

$$(n_1 l_1 \lambda_1)^{w_1+1} \epsilon_i l_i \lambda_i \rightarrow (n_1 l_1 \lambda_1)^{w_1} \epsilon_e l_e \lambda_e \epsilon_f l_f \lambda_f, \tag{3}$$

where $\epsilon_e = k_e^2/2$ is the ejected electron energy. The configuration-average ionization cross section is given by

$$\sigma_{ion} = \int_0^{E/2} d\epsilon_e \frac{64}{k_i^3 k_e k_f} \frac{(w_1+1)}{S(\lambda_1)} \times \sum_{l_i} \sum_{\lambda_i} \sum_{l_e} \sum_{\lambda_e} \sum_{l_f} [M_d(fe;i1) + M_x(ef;1i) - M_c(fe/ef;1i)], \tag{4}$$

where the total energy $E = \epsilon_1 + \epsilon_i = \epsilon_e + \epsilon_f$ and the continuum normalization is again chosen as one times a sine function. The scattering terms M are defined in Sec. II C.

C. Scattering terms

The direct scattering term in Eq. (2) is given by

$$M_d(f2;i1) = \sum_{m_1} \sum_{m_2} \sum_{m_i} \sum_{k} \sum_{k'} \frac{(k-q)!}{(k+q)!} \frac{(k'-q')!}{(k'+q')!} \times R^{kq}(\epsilon_f l_f \lambda_f, n_2 l_2 \lambda_2; \epsilon_i l_i \lambda_i, n_1 l_1 \lambda_1) \times R^{k'q'}(\epsilon_f l_f \lambda_f, n_2 l_2 \lambda_2; \epsilon_i l_i \lambda_i, n_1 l_1 \lambda_1), \tag{5}$$

where $q = |m_2 - m_1| \leq k$ and $q' = |m_2 - m_1| \leq k'$. The exchange scattering term in Eq. (2) is given by

$$M_x(2f;i1) = \sum_{m_1} \sum_{m_2} \sum_{m_i} \sum_{k} \sum_{k'} \frac{(k-q)!}{(k+q)!} \frac{(k'-q')!}{(k'+q')!} \times R^{kq}(n_2 l_2 \lambda_2, \epsilon_f l_f \lambda_f; \epsilon_i l_i \lambda_i, n_1 l_1 \lambda_1) \times R^{k'q'}(n_2 l_2 \lambda_2, \epsilon_f l_f \lambda_f; \epsilon_i l_i \lambda_i, n_1 l_1 \lambda_1), \tag{6}$$

where $q = |m_i - m_2| \leq k$ and $q' = |m_i - m_2| \leq k'$. The cross-scattering term in Eq. (2) is given by

$$M_c(f2/2f;i1) = \sum_{m_1} \sum_{m_2} \sum_{m_i} \sum_{k} \sum_{k'} \frac{(k-q)!}{(k+q)!} \frac{(k'-q')!}{(k'+q')!} \times R^{kq}(\epsilon_f l_f \lambda_f, n_2 l_2 \lambda_2; \epsilon_i l_i \lambda_i, n_1 l_1 \lambda_1) \times R^{k'q'}(n_2 l_2 \lambda_2, \epsilon_f l_f \lambda_f; \epsilon_i l_i \lambda_i, n_1 l_1 \lambda_1), \tag{7}$$

where $q = |m_2 - m_1| \leq k$ and $q' = |m_i - m_2| \leq k'$. In all three scattering terms $\lambda_f = |m_i + m_1 - m_2| \leq l_f$ and the (r,θ) polar coordinate integral is given by

$$R^{kq}(f2;i1) = \int_0^\infty dr_1 \int_0^\infty dr_2 \frac{r_<^k}{r_>^{k+1}} \int_0^\pi d\theta_1 \int_0^\pi d\theta_2 P_q^k(\cos\theta_1) \times P_q^k(\cos\theta_2) u_{\epsilon_f l_f \lambda_f}(r_1,\theta_1) u_{n_2 l_2 \lambda_2}(r_2,\theta_2) \times u_{\epsilon_i l_i \lambda_i}(r_1,\theta_1) u_{n_1 l_1 \lambda_1}(r_2,\theta_2), \tag{8}$$

where $P_q^k(\cos\theta)$ are associated Legendre functions, $u_{nl\lambda}(r,\theta)$ are bound reduced orbitals, and $u_{\epsilon l \lambda}(r,\theta)$ are continuum reduced orbitals. The direct, exchange, and cross-scattering terms in Eq. (4) are also given by Eqs. (5)–(8), following the substitution of $n_2 l_2 \lambda_2 \rightarrow \epsilon_e l_e \lambda_e$.

D. Bound and continuum orbitals

The spatial part of the single-particle wave function for each bound and continuum orbital is given by

$$\psi(r,\theta,\phi) = \frac{u(r,\theta)}{r\sqrt{\sin\theta}} \frac{e^{im\phi}}{\sqrt{2\pi}}. \tag{9}$$

The reduced orbital $u(r,\theta)$ is represented on a uniform mesh in both r and θ. The bound reduced orbitals may be generated by available numerical Hartree-Fock programs for diatomic molecules [21], with conversion to the uniform mesh in (r,θ) center-of-mass polar coordinates. The continuum reduced orbitals are found by solution of a variationally derived [22] single-particle Schrödinger equation given by

$$(Ku)_{i,j} + V_{i,j} u_{i,j} = \epsilon u_{i,j}, \tag{10}$$

where $u_{i,j} = u(r_i,\theta_j)$ is the representation of the reduced orbital on the lattice. With low-order finite differences the kinetic energy operator is given by

$$(Ku)_{i,j} = -\frac{1}{2} \frac{(c_i u_{i+1,j} + c_{i-1} u_{i-1,j} - \bar{c}_i u_{i,j})}{\Delta r^2} - \frac{1}{2r_i^2} \frac{(d_j u_{i,j+1} + d_{j-1} u_{i,j-1} - \bar{d}_j u_{i,j})}{\Delta\theta^2}, \tag{11}$$

where

$$c_i = \frac{r_{i+1/2}^2}{r_i r_{i+1}},$$

$$\bar{c}_i = \frac{(r_{i+1/2}^2 + r_{i-1/2}^2)}{r_i^2},$$

$$d_j = \frac{\sin\theta_{j+1/2}}{\sqrt{\sin\theta_j \sin\theta_{j+1}}},$$

$$\bar{d}_j = \frac{(\sin\theta_{j+1/2} + \sin\theta_{j-1/2})}{\sin\theta_j}. \quad (12)$$

The potential energy operator may be separated into the components

$$V = V_{nuclear} + V_{centrifugal} + V_{direct} + V_{exchange}. \quad (13)$$

The static nuclear term is given by

$$V_{nuclear}(r,\theta) = -\frac{Z_1}{\sqrt{r^2 + R_1^2 - rR_1\cos\theta}} - \frac{Z_2}{\sqrt{r^2 + R_2^2 + rR_2\cos\theta}}, \quad (14)$$

where Z_1 and Z_2 are the nuclear atomic numbers and $R = R_1 + R_2$ is the internuclear separation. The centrifugal term is given by

$$V_{centrifugal}(r,\theta) = \frac{m^2}{2r^2\sin^2\theta}, \quad (15)$$

while the direct Hartree term $V_{direct}(r,\theta)$ and the local density exchange term $V_{exchange}(r,\theta)$ are constructed from previously calculated Hartree-Fock bound orbitals.

The discrete Schrödinger equation (10) may be cast as a system of linear equations $\mathbf{Au}=\mathbf{b}$. The matrix $\mathbf{A}$ is block tridiagonal and is solved by standard LU decomposition. The large-r boundary condition is given by

$$u_{\epsilon l\lambda}(r_{max},\theta) = P_{\epsilon l}(r_{max})\sqrt{2\pi\sin\theta}\,Y_{lm}(\theta,\phi=0), \quad (16)$$

where r_{max} is such that $\epsilon \gg |V(r_{max},\theta)|$ for all θ and $Y_{lm}(\theta,\phi)$ is a spherical harmonic. The reduced radial orbital in the WKB approximation is given by

$$P_{\epsilon l}(r_{max}) = \sqrt{\frac{k}{\zeta(r_{max})}}\sin\Theta(r_{max}), \quad (17)$$

where

$$\Theta(r) = kr - \frac{l\pi}{2} + \frac{q}{k}\ln(2kr) + \sigma_l + \delta_l,$$

$$\zeta(r) = \frac{d\Theta(r)}{dr}, \quad (18)$$

q is the asymptotic charge, σ_l is the Coulomb phase shift, and δ_l is a non-Coulomb phase shift. As $r_{max}\to\infty$, $P_{\epsilon l}(r_{max})$ goes to one times a sine function. As warned by Tully and Berry [13], strong l mixing may occur for unfortunate choices of r_{max}. Our safeguard procedure is to solve every continuum orbital at a succession of different values of r_{max}, until the solution has the correct number of $(l-\lambda)$ angular nodes.

III. RESULTS

To test the molecular configuration-average distorted-wave (CADW) method, we first calculated electron-impact excitation cross sections for H_2^+ at both $R=0.0$ and $R=2.0$. Reduction of Eqs. (2) and (5)–(7) for the $1s\sigma\to 2p\sigma$ transition with $\lambda_i=0$ yields

$$\sigma_{exc} = \frac{16\pi}{k_i^3 k_f}\sum_{l_i}\sum_{l_f}\sum_{k}\sum_{k'} \times [R^{k0}(\epsilon_f l_f 0, 2p0; \epsilon_i l_i 0, 1s0)R^{k'0}(\epsilon_f l_f 0, 2p0; \epsilon_i l_i 0, 1s0) + R^{k0}(2p0, \epsilon_f l_f 0; \epsilon_i l_i 0, 1s0)R^{k'0}(2p0, \epsilon_f l_f 0; \epsilon_i l_i 0, 1s0) - R^{k0}(\epsilon_f l_f 0, 2p0; \epsilon_i l_i 0, 1s0)R^{k'0}(2p0, \epsilon_f l_f 0; \epsilon_i l_i 0, 1s0)], \quad (19)$$

with similar expressions for $\lambda_i \neq 0$. The reduction of the same equations for the $1s\sigma\to 2p\pi$ transition with $\lambda_i=0$ yields

$$\sigma_{exc} = \frac{32\pi}{k_i^3 k_f}\sum_{l_i}\sum_{l_f}\sum_{k}\sum_{k'}\frac{(k-1)!}{(k+1)!}\frac{(k'-1)!}{(k'+1)!} \times [R^{k1}(\epsilon_f l_f 1, 2p1; \epsilon_i l_i 0, 1s0)R^{k'1}(\epsilon_f l_f 1, 2p1; \epsilon_1 l_i 0, 1s0) + R^{k1}(2p1, \epsilon_f l_f 1; \epsilon_i l_i 0, 1s0)R^{k'1}(2p1, \epsilon_f l_f 1; \epsilon_i l_i 0, 1s0) - R^{k1}(\epsilon_f l_f 1, 2p0; \epsilon_i l_i 0, 1s0)R^{k'1}(2p1, \epsilon_f l_f 1; \epsilon_i l_i 0, 1s0)], \quad (20)$$

with similar expressions for $\lambda_i \neq 0$. The $1s\sigma$, $2p\sigma$, and $2p\pi$ bound orbitals for H_2^+ at $R=0.0$ and $R=2.0$ are from the classic tables of Bates *et al.* [23], with conversion to the uniform mesh in (r,θ) center-of-mass polar coordinates. The $\epsilon l\lambda$ continuum orbitals are calculated using Eq. (10) with the direct and exchange potentials of Eq. (13) set to zero—i.e., Coulomb partial waves.

The configuration-average distorted-wave calculations for the excitation and ionization of H_2^+ employed a (1000, 100) lattice with the radial coordinate from $0.0\to 20.0$ spanned by a uniform mesh $\Delta r=0.02$ and the polar coordinate from $0\to\pi$ spanned by a uniform mesh $\Delta\theta=(0.01)\pi$. The angular and magnetic quantum numbers spanned $l_i=0\to 10$, $\lambda_i=0\to 4$, and $l_f=0\to 10$ for excitation and, in addition, $l_e=0\to 4$ and $\lambda_e=0\to 4$ for ionization. For calculation at relatively high incident electron energy, simple extrapolation procedures are used to estimate cross sections for $l_i>10$ and $\lambda_i>4$. A simple parallelization over both l_i and λ_i was employed for the running of the excitation code, while, in addition, a further parallelization over both l_e and λ_e was employed for the running of the ionization code.

Electron-impact excitation cross sections for H_2^+ at $R=0.0$ calculated using the molecular CADW method are presented in Fig. 1. The results for the $1s\sigma\to 2p\sigma$ transition are shown as the connected squares, and the results for the $1s\sigma\to 2p\pi$ transition are shown as the connected circles. The sum of the cross sections for the two transitions is found to be in good agreement with the electron-impact excitation cross section for the $1s\to 2p$ transition in He^+ calculated using the atomic CADW method [6] with Coulomb waves, shown in Fig. 1 as the solid curve.

Electron-impact excitation cross sections for H_2^+ at $R=2.0$ are presented in Figs. 2 and 3. The results for the

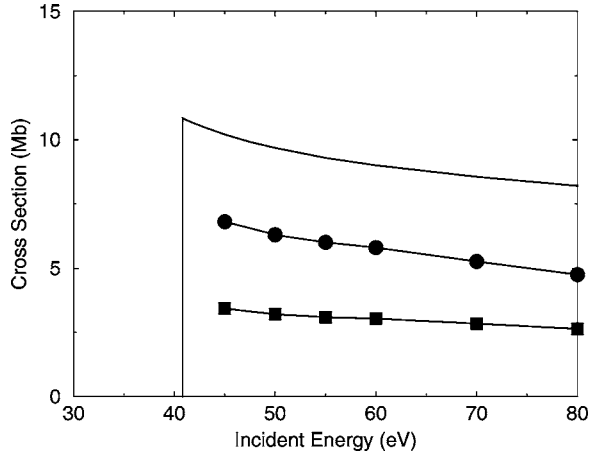

FIG. 1. Electron-impact excitation of H_2^+ at $R=0.0$. Solid curve: $1s \rightarrow 2p$ atomic distorted-wave results. Connected squares: $1s\sigma \rightarrow 2p\sigma$ molecular distorted-wave results. Connected circles: $1s\sigma \rightarrow 2p\pi$ molecular distorted-wave results (1.0 Mb $=1.0\times10^{-18}$ cm^2).

$1s\sigma \rightarrow 2p\sigma$ transition are again shown as the connected squares, and the results for the $1s\sigma \rightarrow 2p\pi$ transition are again shown as the connected circles. The reversal of strengths of the cross sections for the two transitions in going from $R=0.0$ to $R=2.0$ is in keeping with previous molecular plane-wave Born calculations [16], shown in Figs. 2 and 3 as the solid curves. Molecular R-matrix calculations [18] for the transition $1s\sigma \rightarrow 2p\sigma$ are also shown in Fig. 2 as the connected diamonds. In contrast to the molecular plane-wave Born results, the molecular Coulomb-wave cross sections are finite at the excitation threshold, in agreement with the molecular R-matrix results.

To further test the molecular configuration-average distorted-wave method, we calculated electron-impact ionization cross sections for H_2^+ at $R=0.0$ and $R=2.0$. Reduction of Eqs. (4)–(7) for $1s\sigma$ ionization with $\lambda_i=0$ and $\lambda_e=0$ yields

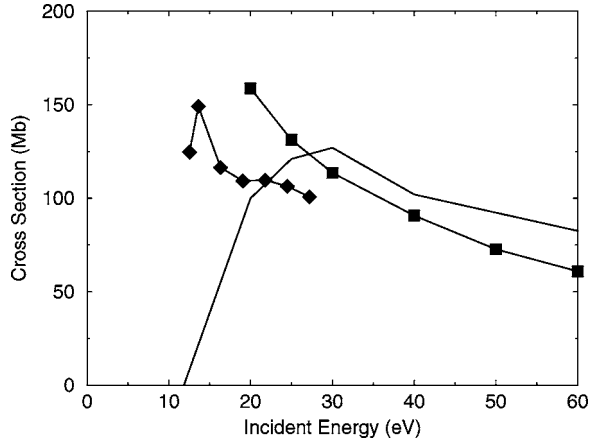

FIG. 2. Electron-impact excitation of H_2^+ at $R=2.0$. Solid curve: $1s\sigma \rightarrow 2p\sigma$ molecular plane-wave Born results [16]. Connected squares: $1s\sigma \rightarrow 2p\sigma$ molecular distorted-wave results. Connected diamonds: $1s\sigma \rightarrow 2p\sigma$ molecular R-matrix results [18] (1.0 Mb $=1.0\times10^{-18}$ cm^2).

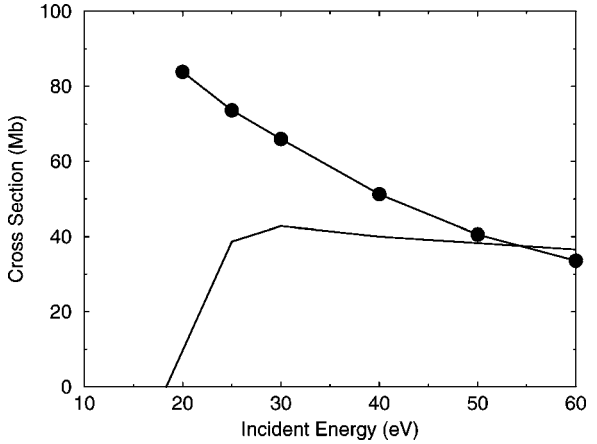

FIG. 3. Electron-impact excitation of H_2^+ at $R=2.0$. Solid curve: $1s\sigma \rightarrow 2p\pi$ molecular plane-wave Born results [16]. Connected circles: $1s\sigma \rightarrow 2p\pi$ molecular distorted-wave results (1.0 Mb $=1.0\times10^{-18}$ cm^2).

$$\sigma_{ion} = \int_0^{E/2} d\epsilon_e \frac{32}{k_i^3 k_e k_f} \sum_{l_i} \sum_{l_e} \sum_{l_f} \sum_{k} \sum_{k'} \times [R^{k0}(\epsilon_f l_f 0, \epsilon_e l_e 0; \epsilon_i l_i 0, 1s0) R^{k'0}(\epsilon_f l_f 0, \epsilon_e l_e 0; \epsilon_i l_i 0, 1s0) + R^{k0}(\epsilon_e l_e 0, \epsilon_f l_f 0; \epsilon_i l_i 0, 1s0) R^{k'0}(\epsilon_e l_e 0, \epsilon_f l_f 0; \epsilon_i l_i 0, 1s0) - R^{k0}(\epsilon_f l_f 0, \epsilon_e l_e 0; \epsilon_i l_i 0, 1s0) R^{k'0}(\epsilon_e l_e 0, \epsilon_f l_f 0; \epsilon_i l_i 0, 1s0)], \quad (21)$$

with similar expressions for $\lambda_i \neq 0$ and $\lambda_e \neq 0$.

Electron-impact ionization cross sections for H_2^+ at $R=0.0$ calculated using the molecular CADW method are presented in Fig. 4. The results for the $1s\sigma$ cross section are shown as connected squares and are in very good agreement with the electron-impact $1s$ ionization cross sections for He^+ calculated using the atomic CADW method [6] with Coulomb waves, shown in Fig. 4 as the solid curve. Both

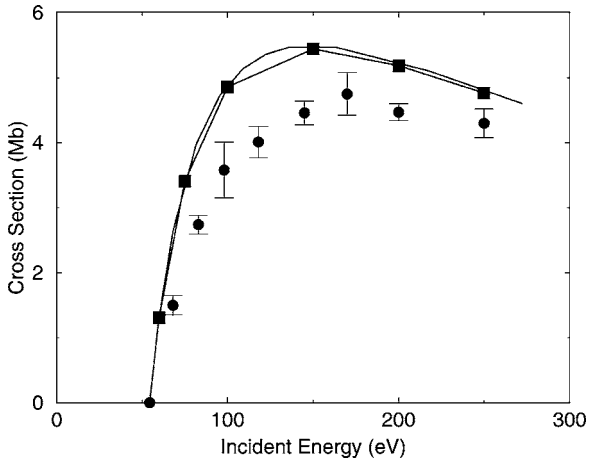

FIG. 4. Electron-impact ionization of H_2^+ at $R=0.0$. Solid curve: $1s$ atomic distorted-wave results. Connected squares: $1s\sigma$ molecular distorted-wave results. Solid circles with error bars: experimental measurements [19] (1.0 Mb$=1.0\times10^{-18}$ cm^2).

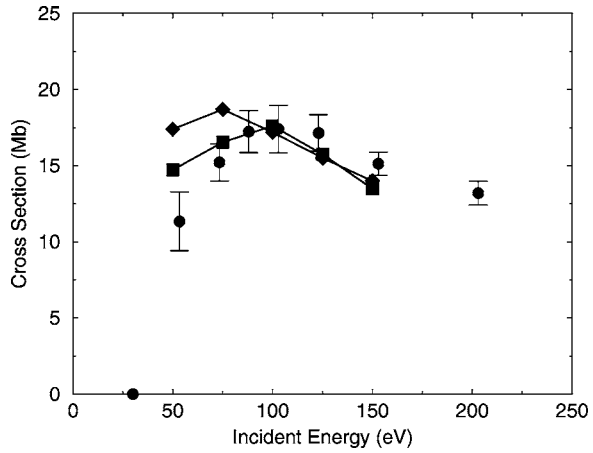

FIG. 5. Electron-impact ionization of H_2^+ at $R=2.0$. Connected squares: $1s\sigma$ molecular distorted-wave results. Connected diamonds: $1s\sigma$ molecular distorted-wave results [17]. Solid circles with error bars: experimental measurements [20] (1.0 Mb $=1.0\times10^{-18}$ cm^2).

Coulomb-wave calculations are higher than the experimental measurements [19] for He^+, shown as the solid circles with error bars. However, more advanced atomic scattering methods, like the convergent close-coupling [24] and the time-dependent close-coupling [25] methods, yield ionization cross sections that are in excellent agreement with the experimental measurements.

Electron-impact ionization cross sections for H_2^+ at $R=2.0$ are presented in Fig. 5. The results for the $1s\sigma$ cross section are again shown as the connected squares. The strength of the ionization cross section has noticeably increased in going from $R=0.0$ to $R=2.0$. Previous molecular distorted-wave results [17] for the $1s\sigma$ cross section, generated in prolate spheroidal coordinates, are shown in Fig. 5 as the connected diamonds. At incident electron energies just above the ionization threshold, both molecular distorted-wave calculations are somewhat higher than the experimental measurements [20], again shown as the solid circles with error bars.

IV. SUMMARY

In conclusion, we have developed a configuration-average distorted-wave method to calculate electron-impact excitation and ionization cross sections for diatomic molecules and their ions. For H_2^+ at $R=0.0$, the molecular CADW results are in very good agreement with atomic CADW results for selected excitation and ionization cross sections of He^+. For H_2^+ at $R=2.0$, the molecular CADW results are in reasonable agreement with previous molecular distorted-wave and R-matrix results for selected excitation and ionization cross sections.

We look forward to applying the molecular CADW method to calculate excitation and ionization processes in a wide variety of diatomic molecules and their ions. For other diatomic molecules, only the bound and continuum orbitals change, while the general collision cross section expressions of Eqs. (1)–(8) and the corresponding computer programs remain exactly the same. The bound orbitals, extracted from existing Hartree-Fock computer programs, will be used in the radial matrix elements of Eq. (8) and will also be used to construct the direct and local exchange potentials of Eq. (13) needed to calculate the continuum orbitals.

We also look forward to applying the molecular CADW method to help develop the application of the molecular time-dependent close-coupling (TDCC) method [5] to electron-molecule scattering processes. An obvious first step will be a molecular TDCC investigation of the electron ionization of H_2^+ at incident energies just above threshold. A second step will be the electron ionization of H_2 in a frozen-core approximation to compare with current R-matrix pseudostate calculations and experiment.

ACKNOWLEDGMENTS

This work was supported in part by grants from the U.S. Department of Energy. Computational work was carried out at the National Energy Research Scientific Computing Center in Oakland, California, and at the National Center for Computational Sciences in Oak Ridge, Tennessee.

[1] *Atomic and Molecular Processes in Fusion Plasmas*, edited by R. K. Janev (Plenum, New York, 1995).
[2] *Computational Methods for Electron-Molecule Collisions*, edited by W. M. Huo and F. A. Gianturco (Plenum, New York, 1995).
[3] J. D. Gorfinkiel and J. Tennyson, J. Phys. B **37**, L343 (2004).
[4] S. Tonzani and C. H. Greene, J. Chem. Phys. **122**, 014111 (2005).
[5] J. Colgan, M. S. Pindzola, and F. Robicheaux, J. Phys. B **37**, L377 (2004).
[6] M. S. Pindzola, D. C. Griffin, and C. Bottcher, in *Atomic Processes in Electron-ion and Ion-ion Collisions*, edited by F. Brouillavd, Vol. 145 of *NATO Advanced Study Institute, Series B: Physics* (Plenum, New York, 1986), p. 75.
[7] J. A. Shaw, M. S. Pindzola, M. Steidl, K. Aichele, U. Hartenfeller, D. Hathiramani, F. Scheuermann, M. Westermann, and E. Salzborn, Phys. Rev. A **63**, 032709 (2001).
[8] K. Aichele, W. Arnold, D. Hathiramani, F. Scheuermann, E. Salzborn, D. M. Mitnik, D. C. Griffin, J. Colgan, and M. S. Pindzola, Phys. Rev. A **64**, 052706 (2001).
[9] S. D. Loch, M. S. Pindzola, C. P. Ballance, D. C. Griffin, D. M. Mitnik, N. R. Badnell, M. G. O'Mullane, H. P. Summers, and A. D. Whiteford, Phys. Rev. A **66**, 052708 (2002).
[10] S. D. Loch, M. S. Pindzola, N. R. Badnell, F. Scheuermann, K. Kramer, K. Huber, and E. Salzborn, Phys. Rev. A **70**, 052714 (2004).
[11] M. S. Pindzola and M. J. Buie, Phys. Rev. A **37**, 3232 (1988).
[12] M. S. Pindzola, D. L. Moores, and D. C. Griffin, Phys. Rev. A

40, 4941 (1989).
[13] J. C. Tully and R. S. Berry, J. Chem. Phys. **51**, 2056 (1969).
[14] J. A. Richards and F. P. Larkins, J. Phys. B **17**, 1015 (1984).
[15] J. A. Richards and F. P. Larkins, J. Phys. B **19**, 1945 (1986).
[16] B. F. Rozsynai, J. Chem. Phys. **47**, 4102 (1967).
[17] F. Robicheaux, J. Phys. B **29**, 779 (1996).
[18] J. Tennyson and C. J. Noble, J. Phys. B **18**, 155 (1985).
[19] B. Peart, D. S. Walton, and K. T. Dolder, J. Phys. B **2**, 1347 (1969).
[20] B. Peart and K. T. Dolder, J. Phys. B **6**, 2409 (1973).
[21] C. J. Gillan, J. Tennyson, and P. G. Burke, in *Computational Methods for Electron-Molecule Collisions*, edited by W. M. Huo and F. A. Gianturco (Plenum, New York, 1995), p. 239.
[22] J. Colgan, M. S. Pindzola, and F. Robicheaux, Phys. Rev. A **68**, 063413 (2003).
[23] D. R. Bates, K. Ledsham, and A. L. Stewart, Philos. Trans. R. Soc. London, Ser. A **246**, 215 (1953).
[24] I. Bray, I. E. McCarthy, J. Wigley, and A. T. Stelbovics, J. Phys. B **26**, L831 (1993).
[25] M. C. Witthoeft, M. S. Pindzola, and J. Colgan, Phys. Rev. A **67**, 032713 (2003).